JOURNAL OF NEUROTRAUMA 29:362–374 (January 20, 2012)

DOI: 10.1089/neu.2011.1942

Lithium Ameliorates Neurodegeneration, Suppresses Neuroinflammation, and Improves Behavioral Performance in a Mouse Model of Traumatic Brain Injury

Fengshan Yu,[1–3] Zhifei Wang,[1] Flaubert Tchantchou,[3] Chi-Tso Chiu,[1] Yumin Zhang,[2,3] De-Maw Chuang[1,2]

Abstract

Although traumatic brain injury (TBI) is recognized as one of the leading causes of death from trauma to the central nervous system (CNS), no known treatment effectively mitigates its effects. Lithium, a primary drug for the treatment of bipolar disorder, has been known to have neuroprotective effects in various neurodegenerative conditions such as stroke. Until this study, however, it has not been investigated as a post-insult treatment for TBI. To evaluate whether lithium could have beneficial effects following TBI, lithium at a dose of 1.5 mEq/kg was administered after injury. Assessed at 3 days and 3 weeks post-injury using hematoxylin and eosin staining, lithium treatment was found to reduce lesion volume. Lithium at doses of 2.0 and 3.0 mEq/kg also significantly reduced lesion volume at 3 days after injury, and the therapeutic window was at least 3 h post-injury. TBI-induced neuronal death, microglial activation, and cyclooxygenase-2 induction were all attenuated by lithium at 3 days after injury. In addition, lithium treatment reduced TBI-induced matrix metalloproteinase-9 expression and preserved the integrity of the blood–brain barrier. As for behavioral outcomes, lithium treatment reduced anxiety-like behavior in an open-field test, and improved short- and long-term motor coordination in rotarod and beam-walk tests. Lithium robustly increased serine phosphorylation of glycogen synthase kinase-3β (GSK-3β), suggesting that the underlying mechanisms responsible for lithium's protective effects are triggered by increasing phosphorylation of this kinase and thereby inhibiting its activity. Our results support the notion that lithium has heretofore unrecognized capacity to mitigate the neurodegenerative effects and improve functional outcomes in TBI.

Key words: GSK-3β; lithium; neuroinflammation; neuroprotection; traumatic brain injury

Introduction

In developed countries, traumatic brain injury (TBI) is a leading cause of morbidity and death in young adults (Maas et al., 2008), and the United States alone averages an estimated 1.7 million TBI cases every year (Faul et al., 2010). TBI causes primary injury (mechanical damage to neurons, glia, and vascular structures), followed by secondary injury including excitotoxicity, oxidative stress, neuroinflammation, mitochondrial dysfunction, and axonal degeneration (Loane and Faden, 2010), and the latter is often associated with cognitive and behavioral dysfunction (Bramlett and Dietrich, 2007). Despite extensive studies aimed at finding successful pharmaceutical therapies, however, the FDA has not yet approved a drug for the treatment of TBI (Hall et al., 2010; Margulies and Hicks, 2009).

The complex pathology of TBI suggests that treating it will require an agent capable of interfering with multiple pathways of cell survival or death (Margulies and Hicks, 2009). One such agent is lithium. For more than half a century, lithium has been the primary medication used to treat bipolar disorder. Prolonged use of this drug is even reported to reverse bipolar patients' loss of gray matter volume (Chuang and Manji, 2007; Sassi et al., 2002). In addition, our and other laboratories have found robust neuroprotective effects of lithium in animal models of a variety of neurological and neurodegenerative diseases, including cerebral ischemia, spinal cord injury, Huntington's disease, Alzheimer's disease,

[1]Section on Molecular Neurobiology, National Institute of Mental Health, National Institutes of Health, Bethesda, Maryland.
[2]Center for Neuroscience and Regenerative Medicine, and [3]Department of Anatomy, Physiology and Genetics, Uniformed Services University of the Health Sciences, Bethesda, Maryland.

and amyotrophic lateral sclerosis (Chiu and Chuang, 2010; Quiroz et al., 2010).

Lithium, a direct inhibitor of glycogen synthase kinase-3β (GSK-3β; Klein and Melton, 1996), can also indirectly inhibit this kinase by enhancing serine phosphorylation through activation of the serine/threonine kinase Akt (Beaulieu et al., 2004; Chalecka-Franaszek and Chuang, 1999), the protein kinase A (Jope, 1999), and the protein kinase C (Kirshenboim et al., 2004). Inhibition of GSK-3 results in enhanced expression of several neuroprotective and neurotrophic proteins, such as heat-shock protein 70 (HSP70; Ren et al., 2003), brain-derived neurotrophic factor (BDNF; Yasuda et al., 2009), and Bcl-2 (Liang and Chuang, 2006; Senatorov et al., 2004). By reducing microglial migration, lithium also modulates inflammation and attenuates inflammation-induced neurotoxicity (Beurel et al., 2010; Yuskaitis and Jope, 2009). Despite its well-known and multifaceted neuroprotective/neurotrophic effects, however, lithium has not been investigated as a post-insult treatment for TBI. The effectiveness of post-insult lithium treatment might be more clinically relevant, since it could realistically be administered to human victims.

In this study, we determined the severity of brain injury produced by a controlled cortical impact (CCI) device with different combinations of parameters. The potential therapeutic effects of lithium were then tested in two different CCI injury conditions. Our results indicate that post-insult administration of lithium reduced lesion volume, neuronal degeneration, microglial activation, and upregulation of cyclooxygenase-2 (COX-2). Lithium treatment also attenuated TBI-induced disruption of the blood–brain barrier (BBB) and upregulation of matrix metalloproteinase-9 (MMP-9). Further, lithium administered after TBI improved functional outcomes on multiple behavioral tests. The beneficial effects of lithium in the TBI model are likely due to its ability to inhibit GSK-3β activity.

Methods

TBI induction and lithium treatment

All animals were treated in accordance with guidelines of the Uniformed Services University of the Health Sciences and the National Institutes of Health *Guide for the Care and Use of Laboratory Animals*. A CCI device (Leica, Wetzlar, Germany) was used to induce TBI in 8-week-old male C57BL/6 mice. Briefly, prior to TBI mice were anesthetized with 2.0% isoflurane in O_2 and mounted on a stereotaxic frame (Kopf Instruments, Tujunga, CA). An approximately 4-mm-diameter craniotomy was performed over the left parietal cortex between the bregma and the lambda sutures. The skullcap was carefully removed with no disruption of the dura. The point of impact was identified midway between the lambda and the bregma sutures, as well as midway between the central suture and the left temporalis muscle. The CCI injury was performed using a 3-mm-diameter convex tip set to compress the brain with combinations of velocity at 5.0 m/sec and different levels of deformation of 1.0–2.5 mm (1.0, 1.5, 2.0, and 2.5 mm). The craniotomy was then closed by repositioning the bone flap. A group of sham-injured mice underwent identical craniotomy procedures without CCI injury. Body temperature was maintained at 37 ± 0.5°C using a heating pad coupled to a rectal probe.

Lithium administration and plasma lithium level measurement

Lithium chloride (1.5 mEq/kg dissolved in normal saline; Sigma-Aldrich, St. Louis, MO) or an equal volume of saline was injected intraperitoneal (IP) 15 min after TBI, followed by injections once daily for up to 2 weeks. For the dose-response study, lithium was injected at different doses (1.0, 1.5, 2.0, 3.0, or 5.0 mEq/kg) 15 min after injury, followed by daily injections for 3 days. For the time-course study, lithium (1.5 mEq/kg) was injected 3 or 6 h after TBI, followed by injections once daily for 3 days. Whole blood samples were collected 12 h after the last of the 2-week lithium injections, and plasma lithium levels were measured using inductively coupled plasma/mass spectrometry by Medtox Scientific Inc. (St. Paul, MN; test code 60063).

Evaluation of lesion volume

Lesion volume was measured at 3 days and 3 weeks after CCI injury. Animals were deeply anesthetized and then transcardially perfused with heparin saline followed by 4% formaldehyde. Brains were collected and fixed in the same fixative for 24–48 h and then in 30% sucrose for 24–48 h. Sections 30 μm thick were cut using a cryostat (Leica) starting at 600 μm anterior to the bregma. Serial sections at 540-μm intervals were stained with hematoxylin and eosin (H&E) and scanned with an Epson scanner. Each section was measured for the area of normal H&E staining with ImageJ software from the National Institutes of Health. Cavitation, hemorrhage, or loss of normal H&E staining were considered as lesions. The lesion area was calculated as the area of the contralateral side minus that of the ipsilateral side. The lesion volume of a given animal was calculated according to a previous report with slight modification (Dash et al., 2010), where A stands for the lesion area (mm^2) for each slice, and X stands for the distance (mm) between two sequential slices: $\{0.5A_1 + 0.5(A_1 + A_2) + \ldots + 0.5(A_{n-1} + A_n) + 0.5A_n\}$ X.

Fluoro-Jade B staining

Fluoro-Jade B (FJB) is a fluorescent dye that can be used to label degenerating neurons specifically. This makes it a valuable tool for evaluating neuronal degeneration after TBI (Hall et al., 2008). To perform FJB staining, serial sections at 540-μm intervals were first immersed in a solution containing 1% sodium hydroxide in 80% ethanol for 5 min followed by 2 min in 70% ethanol. Brain sections were then transferred to a solution of 0.06% potassium permanganate and gently shaken for 10 min. After immersion in a 0.0004% FJB solution, the sections were air-dried and cleared in xylene for at least 1 min before mounting with DPX (Sigma-Aldrich). At 20× magnification the FJB-positive cells were counted in the hippocampal dentate gyrus area of all sections from a given animal.

Immunohistochemical analysis

To assess the inflammatory response after injury, sections were first blocked with 5% normal donkey serum, then incubated overnight at 4°C with a monoclonal rat anti-mouse F4/80 antibody (1:50; Abcam, Cambridge, MA), or a polyclonal rabbit anti-COX-2 antibody (1:100; Cayman Chemical, Ann Arbor, MI). The sections were then reacted for 1 h at room temperature with a FITC-conjugated donkey anti-rat

antibody (1:100; Jackson ImmunoResearch Laboratories, West Grove, PA), or a Cy 3-conjugated donkey anti-rabbit secondary antibody (1:100; Jackson ImmunoResearch Laboratories). Finally, the sections were stained with 4,6-diamino-2-phenylindole (DAPI; Sigma-Aldrich), and mounted with Vectashield mounting medium (Vector Laboratories, Burlingame, CA). Sections were visualized via fluorescence microscopy (Olympus, Center Valley, PA). Cell density was measured according to a method previously reported (Clausen et al., 2009; Shein et al., 2009) with slight modifications. Briefly, immunostaining of three sections approximately 50 μm apart at bregma −2.0 mm level from a given animal was performed. For each section, three high-power (40×) photomicrographs were taken in the area adjacent to the injury site. For COX-2 immunostaining, photomicrographs were taken in layer II of the cortex adjacent to the injury site. Positive cells were identified and counted using Adobe Photoshop (Mountain View, CA) software and averaged for a given animal. Cell counting was performed by an observer blinded to treatment status.

Double-fluorescent staining

To study cell-type-specific expression of COX-2, we double-fluorescence stained COX-2 with neuronal nuclear antigen (NeuN for neurons), glial fibrillary acidic protein (GFAP for astrocytes), and F4/80 (for microglia/macrophages). Briefly, the sections were incubated overnight at 4°C with a polyclonal rabbit anti-COX-2 antibody (1:100; Cayman Chemical), together with a biotin conjugated anti-NeuN antibody (1:100; Millipore, Billerica, MA), an Alexa Fluor 488-conjugated mouse GFAP antibody (1:100; Cell Signaling, Danvers, MA), or a monoclonal rat anti-mouse F4/80 antibody (1:50; Abcam). The sections were then incubated with the respective secondary antibodies at room temperature for 1 h. Finally, the sections were stained with DAPI (Sigma-Aldrich) and mounted with Vectashield mounting medium. Sections were visualized via fluorescence microscopy (Olympus) for staining. A confocal laser microscope (Zeiss LSM 510; Carl Zeiss, Oberkochen, Germany) was used to verify the co-localization of NeuN and COX-2 at a thinner slice layer.

Western blotting analysis

Western blotting was performed as previously described (Kim et al., 2007). Brain tissue was collected from the cortex posterior to the bregma on the injury side and sonicated for 30 sec in lysis buffer (T-PER tissue protein extraction reagent; Thermo Scientific, Rockford, IL) with phosphatase inhibitors I and II (Sigma-Aldrich), and protease inhibitor cocktail (Roche Diagnostics, Mannheim, Germany). The lysates were centrifuged at 12,000 rpm for 20 min. Protein concentrations were determined using the BCA method. An aliquot containing 30 μg of protein was loaded to each lane, and proteins were separated by electrophoresis on SDS-polyacrylamide gels of 4–12% (Invitrogen, Carlsbad, CA), followed by transferring to a polyvinylidene difluoride membrane. The membranes were incubated overnight at 4°C with monoclonal rabbit anti-phospho-GSK-3β (1:500; Cell Signaling), monoclonal rabbit anti-total GSK-3β (1:2,000; Cell Signaling), monoclonal rabbit anti-MMP-9 (1:1000; Origene, Rockville, MD), polyclonal rabbit anti-phospho-Akt (1:1000; Cell Signaling), polyclonal rabbit anti-Akt (1:2,000; Cell Signaling), or monoclonal mouse anti-β-actin (1:5000; Sigma-Aldrich) antibodies. The membranes were then incubated with goat anti-rabbit IRDye 800CW-conjugated or goat anti-mouse IRDye 700CW-conjugated secondary antibodies and scanned with an Odyssey machine (LI-COR Biosciences, Lincoln, NE).

Evans blue extravasation

With slight modifications, we used Evans blue extravasation to evaluate the integrity of the BBB (Wang et al., 2011). At 68 h after TBI, 2% Evans blue (Sigma-Aldrich) in saline at 5 mL/kg of body weight was administered through the jugular vein. Four hours later, mice were transcardially perfused with heparin saline to remove the intravascular Evans blue. Both ipsilateral and contralateral hemispheres of the brain were weighed and then homogenized individually in 0.5 mL of 50% trichloroacetic acid. The lysates were further centrifuged at 4000g for 40 min. The supernatant was measured by spectrophotometry at a wavelength of 620 nm. The results were calculated using its standard curve and expressed as μg/g of tissue.

Beam-walk test

To evaluate fine motor coordination, a beam-walk test was performed as previously described (Fox et al., 1998; Loane et al., 2009). The beam-walk device contains a narrow wooden beam 6 mm in width and 120 cm in length suspended about 30 cm above a table. Before surgery, each mouse was trained to walk from one end of the beam to the other. The number of foot faults for the right hindlimb was counted over 50 steps. Animals with a basal level of < 10 faults per 50 steps were selected for the experiment. The beam-walk test was performed on days 1, 3, 7, 14, and 21 post-injury, and the number of foot faults per 50 steps was recorded.

Rotarod test

A rotarod test was used to evaluate motor coordination. For four consecutive days before surgery, the mice received training on a rotarod device (Ugo Basile, Collegeville, PA) with an accelerating protocol. Briefly, the rotarod was accelerated from 4 to 40 rpm in 4 min and maintained at 40 rpm for 1 min. Latency to fall from the device or to cling and rotate for two full rotations was recorded. After surgery, rotarod performance was evaluated on days 1, 3, and 7 post-injury with four trials each day; the animals were given at least 5 min to rest between trials. The best performance of the four trials on each day was recorded as previously reported (Walker et al., 2010).

Open-field test

To evaluate gross motor function, the animals underwent an open-field test 10 days post-TBI. Each mouse was gently placed in the center of an acrylic arena (40×40 cm with black walls) and allowed to explore freely for 10 min. The inner square of 20×20 cm was defined as the center zone, while the remainder of the structure was defined as the peripheral zone. The total distance animals traveled and the time spent in the center zone were video-recorded and analyzed using ANY-Maze software (Stoelting Co., Wood Dale, IL). The open field test was performed on the same group of animals subjected to the beam-walk test under the 2.0 mm condition. All other behavioral tests were performed on different cohorts of animals.

Statistical analysis

All data analyses were carried out using GraphPad Prism software (GraphPad Software, Inc., La Jolla, CA). Two-way repeated measures analysis of variance (ANOVA) with *post-hoc* Bonferroni comparison was used to analyze results of the beam-walk and rotarod tests. One-way ANOVA was used to compare data among multiple groups, and Student's *t*-test was used to compare between two groups. Results were quantified and expressed as mean ± standard error of the mean (SEM). Statistical significance was defined as $p < 0.05$.

Results

Characterization of combinations of velocity and different levels of deformation on the severity of TBI

To characterize the injury severity caused by different levels of impact, we tested four different CCI conditions with velocity at 5 m/sec and various levels of deformation: 1.0, 1.5, 2.0, and 2.5 mm (Fig. 1A and C). In the 2.5-mm injury condition, a lesion was noted in the cortex and the entire hippocampus on the ipsilateral side, as detected by H&E staining. In the 1.5-mm and 2.0-mm injury conditions, a lesion was observed in the cortex and part of the ipsilateral hippocampus. By contrast, in the 1.0-mm condition, a lesion occurred only in the cortex but not in the hippocampus. We chose the 1.5-mm and 2.0-mm injury conditions for our study. The 1.5-mm condition was mainly used for short-term (3 days) experiments, as better tissue preservation was observed compared with the 2.0-mm condition. For long-term (3 weeks) studies and most behavioral tests, we selected the 2.0 mm condition as the optimal injury, because it consistently induced hyperlocomotor activity and anxiety-like behavior in the open-field test.

Post-insult lithium treatment reduces TBI-induced brain lesions in mice

To test whether post-insult lithium treatment reduces TBI-induced brain lesions, we evaluated lesion volume with H&E staining at 3 days post-injury in the 1.5 mm condition, and 3 weeks after injury in the 2.0 mm condition. In the first test (3 days post-injury in the 1.5 mm condition), daily injection with 1.5 mEq/kg lithium chloride decreased lesion volume from $7.26 \pm 0.38\,mm^3$ in the saline-treated group to $4.96 \pm 0.38\,mm^3$ in the lithium-treated group (Fig. 1B and D; $p < 0.01$). Similarly, at 3 weeks after injury in the 2.0 mm condition, post-insult lithium treatment for 2 weeks reduced lesion volume from $14.76 \pm 1.39\,mm^3$ in the saline-treated group to $10.18 \pm 1.03\,mm^3$ in the lithium-treated group (Fig. 1B and D; $p < 0.05$). In both conditions, no lesion was found in the contralateral cerebral hemisphere. The dose-response study showed that lithium at doses of 1.5, 2.0, and 3.0 mEq/kg, all significantly reduced lesion volume at 3 days after injury, while lithium did not reduce lesion volume at doses of 1.0 or 5.0 mEq/kg (Fig. 1E). The time-course study showed that lithium still significantly reduced lesion volume when administered 3 but not 6 h post-injury (Fig. 1F). Therefore, the lowest effective dose (1.5 mEq/kg) was chosen for this study. The plasma lithium level was 0.14 ± 0.01 mEq/mL 12 h after the last of 2-week lithium injections ($n = 4$).

Lithium treatment decreases the number of degenerating neurons in the dentate gyrus of TBI mice

To evaluate neurodegeneration in the hippocampus, we used FJB staining, a valuable tool for measuring neuronal degeneration after TBI (Hall et al., 2008). The hippocampus is a vulnerable area to central nervous system (CNS) injuries, and selective death of newborn neurons in the hippocampal dentate gyrus has been reported after TBI (Gao et al., 2008). Three days after TBI, the number of FJB-positive cells in the dentate gyrus was significantly reduced in the lithium-treated group, compared with the saline-treated group. The average number of FJB-positive cells in the dentate gyrus was 232 ± 34 in the saline-treated group, and 98 ± 4 in the lithium-treated group (Fig. 2; $p < 0.05$). No FJB-positive cells were found in the dentate gyrus of the sham-injured animals.

Lithium suppresses TBI-induced neuroinflammation

Recognizing that neuroinflammation plays an important role in the pathogenesis of TBI, we used F4/80 immunostaining to study lithium's effect on microglial activation. In sham-injured animals, the ipsilateral cortex contained no positive cells for F4/80 (Fig. 3B). By contrast, in animals measured 3 days post-TBI, the levels of F4/80-labelled microglia/macrophages around the injury site in the ipsilateral cortex increased markedly. In the saline-treated group, average microglia/macrophage cell density rose to 466 ± 32 cells/mm^2 (Fig. 3C and 3I). In animals treated with lithium, however, levels of microglia/macrophages declined to 228 ± 26 cells/mm^2, or less than half of the levels in the untreated group (Fig. 3D and I; $p < 0.01$).

COX-2 is the rate-limiting enzyme that catalyzes the metabolism of arachidonic acid into inflammatory prostaglandins (Andreasson, 2010). When compared with the sham-injured group (Fig. 3F), TBI robustly increased the expression of COX-2 in the cortex adjacent to the injury site (Fig. 3G), while in the lithium-treated group, the expression of COX-2 was suppressed (Fig. 3H). In the saline-treated group, the average density of COX-2-positive cells in the cortex area was 855 ± 103 cells/mm^2, while in the lithium-treated group, it decreased to 414 ± 97 cells/mm^2 (Fig. 3J; $p < 0.05$).

To further explore cell-type-specific expression of COX-2, we performed double-fluorescence staining using COX-2 and selective markers from different cell types. We found that COX-2 was mainly expressed in neurons located in the area adjacent to the injury site (Fig. 4 upper panel), and there was no co-localization of COX-2 with markers for astrocytes (Fig. 4 lower panel and Supplementary Fig. 1; see online supplementary material at http://www.liebertonline.com), or microglia (Supplementary Fig. 2; see online supplementary material at http://www.liebertonline.com). The expression of COX-2 in NeuN-positive cortical neurons was further verified by confocal microscopy (Supplementary Fig. 3; see online supplementary material at http://www.liebertonline.com).

Lithium attenuates BBB breakdown and MMP-9 expression after TBI

To investigate BBB integrity, we detected Evans blue extravasation at 3 days after TBI. The extravasation of Evans blue in ipsilateral brain tissue was markedly increased in the saline-treated group ($4.94 \pm 0.23\,\mu g/g$ tissue), and this was

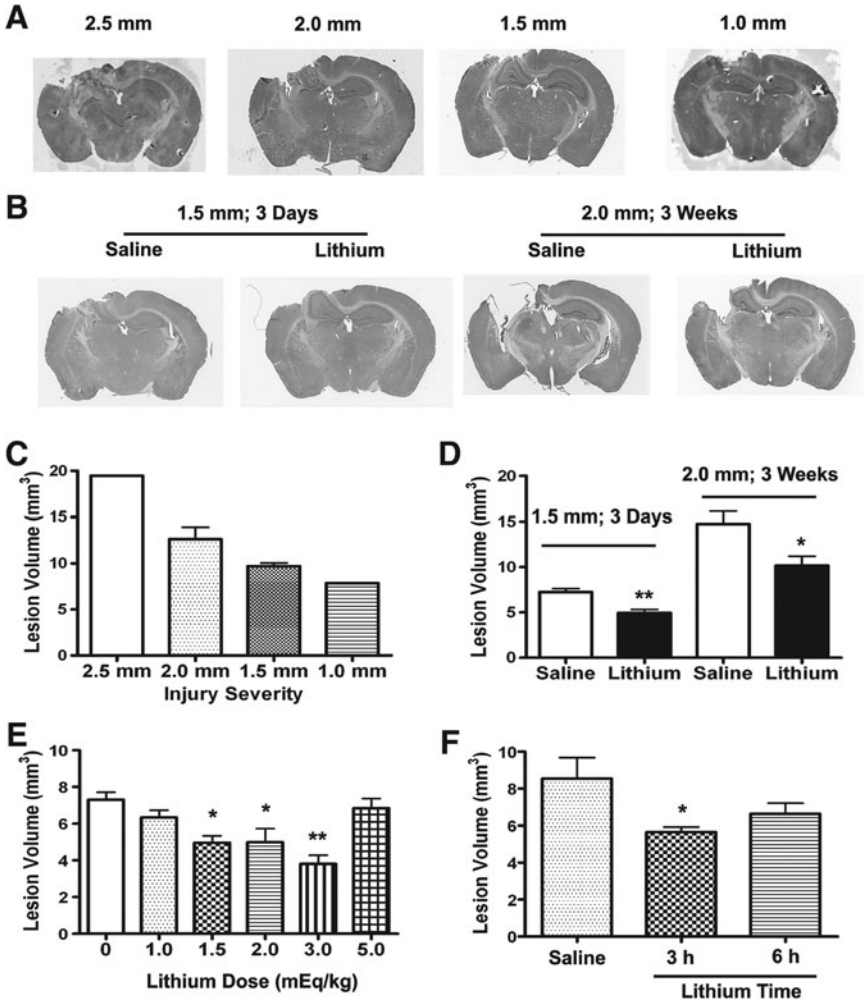

FIG. 1. Post-insult lithium treatment reduces controlled cortical impact (CCI)-induced brain lesion in traumatic brain injury (TBI) mice. Hematoxylin and eosin (H&E) staining was performed to evaluate lesion volume 3 days and 3 weeks after injury. Three days post-injury, a lesion was noted in the ipsilateral cortex in all injury conditions. In addition, a lesion was observed in the entire ipsilateral hippocampus in the 2.5-mm group. In the 2.0-mm and 1.5-mm groups, a lesion was noted in part of the ipsilateral hippocampus, but no such lesion was noted in the hippocampus in the 1.0-mm group (**A**). Three days post-injury, lesion volume as measured by National Institutes of Health (NIH) ImageJ software was correlated with the severity of injury (**C**). Effects of lithium on lesion volume were evaluated by H&E staining on serial sections at 3 days post-injury in the 1.5-mm group, and 3 weeks post-injury in the 2.0-mm group (**B** and **D**). A significant reduction in lesion volume was observed in both conditions ($n = 6$/group for 3 days; $n = 5$/group for 3 weeks; $^*p < 0.05$, $^{**}p < 0.01$, when lithium-treated groups were compared to their respective saline-treated groups). Effects of different lithium doses on lesion volume were evaluated with H&E staining at 3 days after injury (**E**). Different doses of lithium were administered 15 min after injury. At doses of 1.5, 2.0, and 3.0 mEq/kg, lithium significantly reduced lesion volume. At doses of 1.0 or 5.0 mEq/kg, lithium had no effect on lesion volume ($n = 6$/group for the sham and 1.5-mEq/kg groups; $n = 4$/group for the other groups; $^*p < 0.05$). The effects of lithium administered at different time points post-injury were evaluated with H&E staining 3 days after injury (**F**). Lithium at 1.5 mEq/kg was given 3 or 6 h after injury. In the group of animals that received lithium at 3 but not 6 h after injury, the lesion volume was significantly reduced. ($n = 6$/group; $^*p < 0.05$). Data are represented as mean ± standard error of the mean.

significantly lower in the lithium-treated group (3.29 ± 0.36 μg/g tissue; Fig. 5A; $p < 0.01$). In the contralateral side of the brain there was only a small amount of Evans blue, with no significant difference between the saline-treated (1.49 ± 0.19 μg/g tissue) and lithium-treated (1.26 ± 0.10 μg/g tissue) groups. We further examined protein levels of MMP-9, an enzyme largely responsible for the degradation of the extracellular matrix proteins that maintain BBB integrity (Rosell et al., 2008). In the ipsilateral cortex 3 days after TBI, levels of MMP-9 in saline-treated animals were enhanced by more than twofold compared with sham-injured animals (Fig. 5B; $p < 0.05$). By contrast, lithium treatment completely blocked this increase (Fig. 5B; $p < 0.05$).

Lithium improves motor coordination after TBI

To evaluate fine motor movement, the beam-walk test was performed for the two selected injury conditions. In both cases, TBI induced a significant increase in the number of foot faults, with a trend toward recovery in both the lithium- and

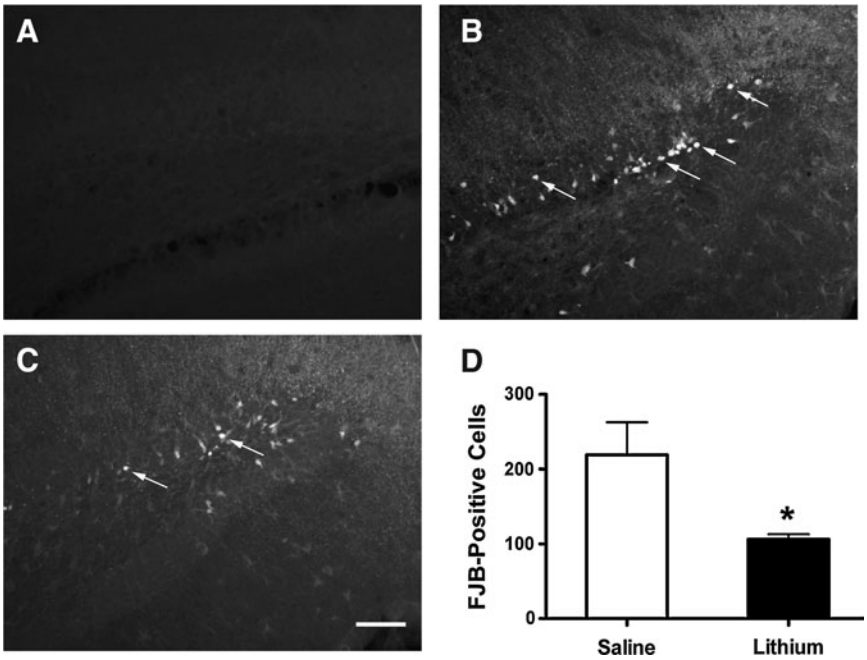

FIG. 2. Post-insult lithium treatment decreases the number of degenerating neurons in the dentate gyrus of traumatic brain injury (TBI) mice. Fluoro-Jade B (FJB) staining was performed to evaluate neuronal degeneration. No FJB-positive cells were observed in the dentate gyrus of the sham-injured group (**A**). Three days post-injury, numerous FJB-positive cells were visualized as staining (arrows in **B**). Fewer FJB-positive cells were observed in response to lithium treatment (**C**). Quantitative analysis showed that the number of FJB-positive cells was significantly reduced in the lithium-treated group, compared with the saline-treated group (**D**; $n = 5$/group; $^*p < 0.05$; scale bar = 50 μm). Data are represented as mean ± standard error of the mean.

saline-treated groups. At 7 days after injury in the 1.5-mm condition, the number of foot faults was significantly reduced, from 46 ± 3 in the saline-treated group to 31 ± 3 in the lithium-treated group (Fig. 6A; $p < 0.01$). At 14 days after injury, the number of foot faults was markedly reduced, from 34 ± 3 in the saline-treated group to 17 ± 2 in the lithium-treated group (Fig. 6A; $p < 0.01$). At 21 days after injury, the number of foot faults was significantly decreased, from 35 ± 3 in the saline-treated group to 13 ± 3 in the lithium-treated group (Fig. 6A; $p < 0.01$). Similar results were also found in TBI induced under the 2.0-mm CCI condition (Fig. 6B). The foot faults were 44 ± 4 (saline) and 30 ± 4 (lithium) at 14 days post-TBI, and were 44 ± 2 (saline) and 29 ± 4 (lithium) at 21 days post-TBI (Fig. 6B; $p < 0.01$). Therefore treatment with lithium demonstrably improves and speeds recovery of fine motor coordination.

The rotarod test was used to evaluate motor coordination in the 1.5 mm CCI paradigms of TBI. At 1 day after injury, lithium treatment significantly improved motor coordination by increasing average latency to fall from 109.7 ± 16.41 sec in the saline-treated group to 171.0 ± 9.47 sec in the lithium treated group (Fig. 6C; $p < 0.05$). Note that CCI-induced deficits in rotarod performance at 1 and 3 days post-injury were largely recovered at 7 days after injury (Fig. 6C; $p < 0.01$).

Lithium attenuates TBI-induced hyper-locomotor activity and anxiety-like behaviors

The open-field test was used to evaluate gross motor function and anxiety-like behaviors in the 2.0 mm injury condition 10 days after injury. We found that after TBI, mice traveled a significantly longer distance (34.89 ± 2.26 m) than those in the sham-injured group (26.47 ± 2.25 m; Fig. 7B; $p < 0.05$), but lithium treatment robustly reduced the distance traveled of the injured mice to nearly the same level as that of the sham-injured group (27.76 ± 1.70 m; Fig. 7B; $p < 0.05$). To measure the anxiety levels in TBI mice, we tracked the amount of time they spent in the center zone, since spending less time in the center zone has been shown to indicate an anxiety-like behavior in mice (Prut and Belzung, 2003). We found that TBI mice spent less time (21.45 ± 3.29 sec) in the center zone than did sham-injured mice (41.37 ± 4.50 sec; Fig. 7C; $p < 0.01$). Lithium treatment significantly increased the time TBI mice spent in the center zone, to 32.33 ± 3.32 sec (Fig. 7C; $p < 0.05$). These results support the finding that lithium attenuates hyper-locomotor activity and anxiety-like behaviors after TBI.

Lithium increases GSK-3β phosphorylation after TBI

Mounting evidence supports the observation that lithium inhibits GSK-3β, both directly and indirectly, and that GSK-3 inhibition underlies much of the actions and effects of this drug (Chiu and Chuang, 2010; Li and Jope, 2010). To study the effects of lithium and the role of GSK-3β inhibition, we used Western blotting to assess the phosphorylation of GSK-3β (p-GSK-3β) at 3 days after TBI. Although there was no significant difference in the levels of p-GSK-3β at Ser 9 between the TBI and sham-injured groups, lithium treatment induced a more than threefold increase in the serine phosphorylation of GSK-3β (Fig. 8A; $p < 0.05$), while protein levels of total GSK-3β (t-GSK-3β) were unchanged (Fig. 8A). By examining the phosphorylation of Akt (p-Akt), one of the upstream serine/threonine kinases that phosphorylate and inhibit GSK-3, we

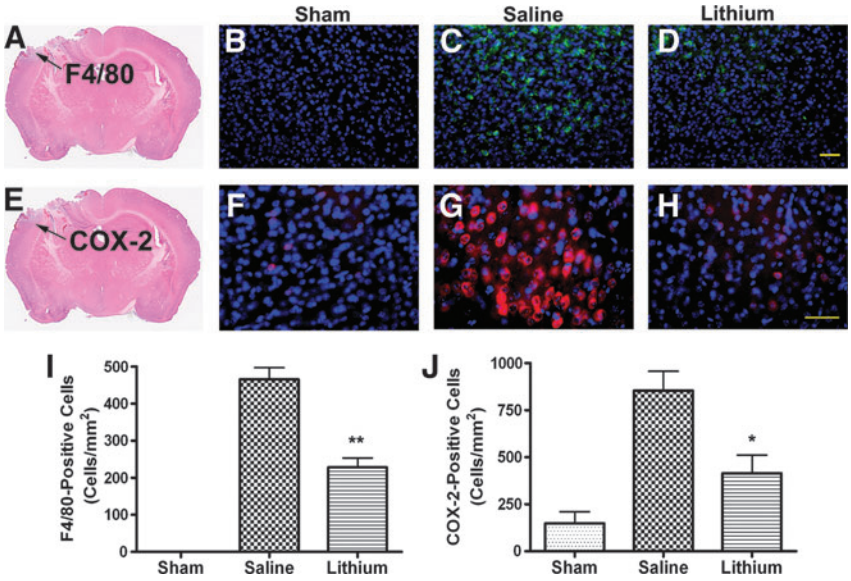

FIG. 3. Lithium suppresses microglial activation and cyclooxygenase-2 (COX-2) expression in the cortex of traumatic brain injury (TBI) mice. Representative photomicrographs of F4/80 staining for microglia activation (**B**–**D**) and COX-2 expression (**F**–**H**) in the cortex adjacent to the injury area are shown. The area of F4/80 and COX-2 staining is indicated by an arrow in hematoxylin and eosin (H&E) staining (**A** and **E**). No F4/80-positive cells were found in the cortex of the sham-injured animals (**B**). Three days post-TBI, the levels of F4/80-positive cells were dramatically increased in the cortex surrounding the lesion site in the saline-treated group (**C**), compared with the lithium-treated group (**D**). Quantitative data showed a significant reduction in the number of F4/80-positive cells in the lithium-treated group compared to the saline-treated group (**I**; $n = 6$/group; $^{**}p < 0.01$). Few COX-2-positive cells were seen in the cortex of the sham-injured animals (**F**). Three days post-injury, a robust increase in COX-2 expression was seen in the cortex surrounding the lesion site in the saline-treated group (**G**). Fewer COX-2-positive cells were seen in this area following lithium treatment (**H**). Quantitative data reflected a significant reduction in the number of COX-2-positive cells in the lithium-treated group, compared with the saline-treated group (**J**; $n = 6$/group; $^{*}p < 0.05$; scale bar = 50 μm). Nuclei were stained with 4,6-diamino-2-phenylindole, as shown with blue fluorescence. Data are represented as mean ± standard error of the mean.

found a significant increase in p-Akt at Ser 473 in the lithium-treated group compared with the sham-injured group (Fig. 8B; $p < 0.05$), but no significant difference between the sham-injured and the saline-treated groups was observed. In all groups, the protein levels of total Akt (t-Akt) were also unaltered (Fig. 8B). These results suggest that the phosphorylation and subsequent inhibition of GSK-3β likely contribute to lithium's beneficial effects against TBI.

Discussion

To our knowledge, this is the first study to demonstrate that post-insult treatment with lithium has beneficial effects in a mouse model of TBI. Specifically, we found that IP delivery of lithium (starting at 15 min after injury and followed by daily injection for 3 days or 2 weeks) significantly reduced lesion volume at 3 days and 3 weeks, and attenuated neuronal

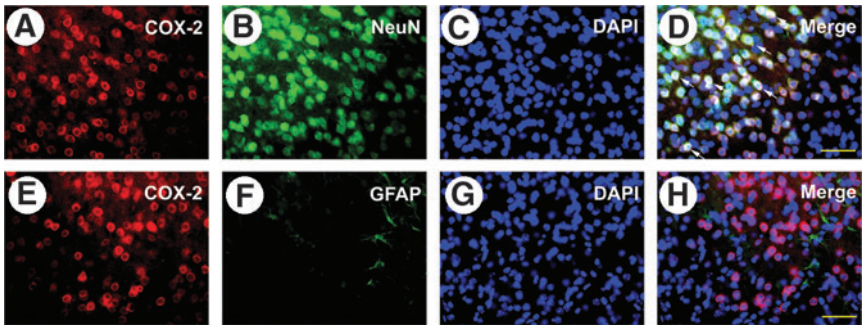

FIG. 4. A majority of cyclooxygenase-2 (COX-2)-positive cells are neuronal nuclear antigen (NeuN)-positive neurons. Representative photomicrographs of double immunofluorescence staining of COX-2 with NeuN or glial fibrillary acidic protein (GFAP) are shown. Upper panels: Double staining of COX-2 (red; **A**) and NeuN (green; **B**) at 3 days after injury. The merged image showed yellow fluorescence, meaning that COX-2 staining is co-localized with NeuN (**D**; arrows). Lower panels: Double staining of COX-2 (red; **E**) and GFAP (green; **F**) at 3 days after injury. The merged image did not show co-localization of COX-2 and GFAP (**H**). In fact, few GFAP-positive cells were detected in the area where COX-2-positive cells were abundant. 4,6-Diamino-2-phenylindole (DAPI; blue; **C** and **G**) was used to stain the nuclei (scale bar = 50 μm).

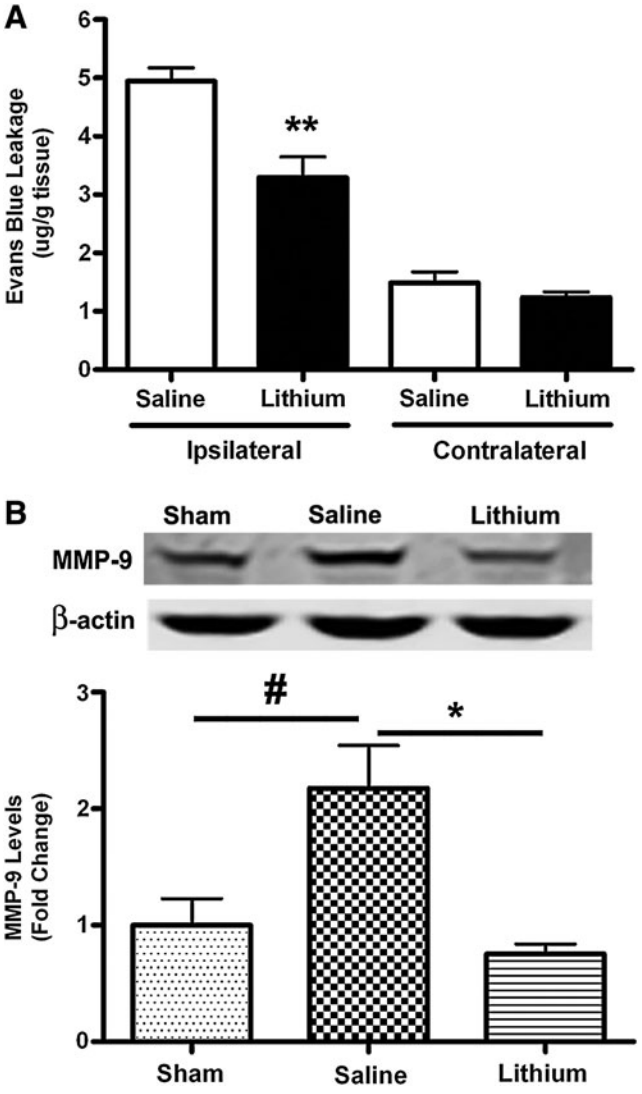

FIG. 5. Lithium reduces blood–brain barrier (BBB) disruption and matrix metalloproteinase-9 (MMP-9) expression after traumatic brain injury (TBI). BBB integrity was evaluated by Evans blue extravasation (**A**), and MMP-9 protein levels were assessed by Western blotting analysis (**B**). Increased Evans blue extravasation was noted in the ipsilateral brain in both the saline- and lithium-treated groups at 3 days after TBI, while the lithium-treated group showed significantly lower levels of Evans blue, compared with the saline-treated group (**A**, $n=4$/group; $^{**}p<0.01$). In the contralateral brain, a small amount of Evans blue was detected and no difference was found between the saline- and lithium-treated groups (**A**). Representative Western blots and quantified data showed that MMP-9 protein levels were increased 3 days after TBI in the saline-treated group (**B**; $n=5$ for the sham group; $n=4$ for the saline group; $^{\#}p<0.05$), compared with the sham-injured group. Lithium treatment significantly reduced MMP-9 protein levels (**B**; $n=4$ for the lithium group; $^{*}p<0.05$). Data are represented as mean ± standard error of the mean.

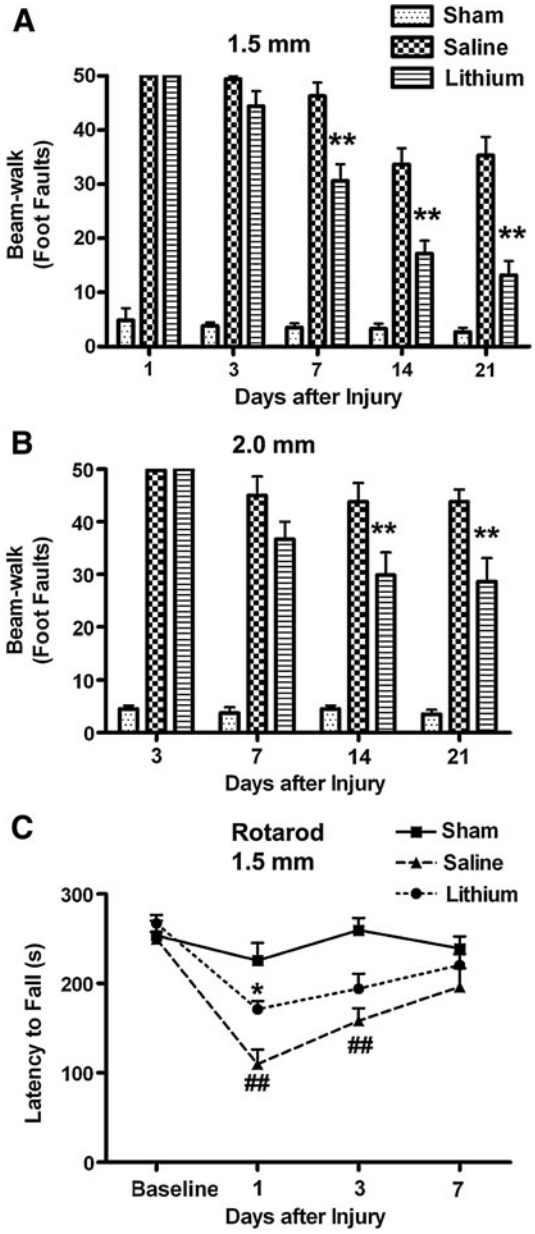

FIG. 6. Lithium markedly improves motor coordination in traumatic brain injury (TBI) mice. TBI increased the number of foot faults in both the saline- and lithium-treated groups under the condition of 1.5 mm (**A**). A slow recovery from 7 to 21 days post-injury was seen in both groups. A significant reduction in the number of foot faults was observed in the lithium-treated group at 7, 14, and 21 days after injury ($n=8$ for the saline group; $n=6$/group for the sham and lithium groups; $^{**}p<0.01$). TBI increased the number of foot faults in both the saline- and lithium-treated groups under the 2.0-mm condition (**B**). A similar slow recovery from 7 to 21 days post-injury was noted in both groups. A significant reduction in the number of foot faults in the lithium-treated group was seen at 14 and 21 days post-injury ($n=6$/group; $^{**}p<0.01$). Under the 1.5 mm condition, a significant decline in rotarod performance was observed in the saline-treated group, compared with the sham-injured group, at 1 and 3 days after injury (**C**; $n=6$/group; $^{\#\#}p<0.01$). Lithium treatment significantly improved rotarod performance 1 day post-injury (**C**; $n=6$ for lithium group; $^{*}p<0.05$). Data are represented as mean ± standard error of the mean.

degeneration in the hippocampal dentate gyrus at 3 days after CCI-induced injury. Lithium treatment also suppressed activation of microglia, induction of COX-2, and disruption of the BBB at 3 days after TBI, giving further proof of the ability of lithium to suppress neuroinflammation after TBI. Finally, the

improved performance on the beam-walk, rotarod, and open-field tests indicates that lithium treatment also improved behavioral outcomes following TBI.

Chronic pre-insult treatment followed by post-insult treatment with lithium has also been shown to reduce lesion volume, ameliorate hippocampal neurodegeneration, attenuate levels of proinflammatory interleukin-1β (IL-1β), and improve Morris water maze performance in a mouse model of TBI (Zhu et al., 2010). However, without long-term pre-insult treatment, post-insult treatment with lithium at a dose of 1.0 mEq/kg failed to show beneficial effects in TBI (Zhu et al., 2010). In contrast, our dose-response study showed that post-insult treatment with lithium at doses of 1.5, 2.0, and 3.0 mEq/kg significantly reduced TBI-induced lesion volume. In addition, treatment with lithium at a dose of 5.0 mEq/kg produced no benefit in reducing lesion volume. These results are consistent with the preclinical and clinical observation that lithium has a relatively narrow dose window, and therefore the lack of neuroprotection at supratherapeutic doses, such as 5 mEq/kg, could be related to its toxic effects (Chiu and Chuang, 2010).

It is well known that neuroinflammation contributes to the pathogenesis of TBI (Loane and Faden, 2010). To evaluate lithium's effect on neuroinflammation, we focused on microglial activation and COX-2 expression. Microglia, which play an important role in the inflammatory response to injury or infection in the brain (Yuskaitis and Jope, 2009), have been found in areas surrounding the injury site from 3 days to 8 weeks after TBI (Yu et al., 2010). Attenuation of microglia activation via inhibition of interleukin-1β (IL-1β) and histone deacetylase inhibition contributes to the neuroprotective effect against TBI (Clausen et al., 2009; Shein et al., 2009). COX is the rate-limiting enzyme responsible for the generation of prostaglandins, which are important mediators of inflammation (Andreasson, 2010). COX-2 is an inducible form of COX expressed in glutamatergic neurons in normal conditions (Niwa et al., 2000). COX-2 is markedly upregulated in animal models of TBI (Ahmad et al., 2008; Kunz et al., 2002, 2006). However, the effects of COX-2 inhibition after TBI are inconsistent. For example, pharmacological inhibition of COX-2 with nimesulide was reported to have beneficial effects against TBI (Cernak et al., 2002), whereas inhibition of this enzyme with another selective inhibitor rofecoxib showed no significant neuroprotection, despite a reduction in the number of TUNEL-positive cells (Kunz et al., 2006). In addition, genetic knockdown of COX-2 had only minor effects in sparing cortical tissue, and had no effect on behavioral outcome after TBI (Kelso et al., 2009). Another report also showed that genetic disruption of COX-2 did not change the lesion volume or alter Morris water maze performance after TBI (Ahmad et al., 2008). The results of the present study suggest that lithium's ability to attenuate microglia activation and COX-2 upregulation may help to reduce neuronal damage following TBI.

BBB disruption, which occurs in hours to days after TBI, is associated with neuroinflammation and cell death in both animal models and patients with head trauma (Shlosberg et al., 2010). Attenuation of BBB disruption in animal models of TBI, spinal cord injury, and cerebral ischemia has been shown to be beneficial (Lotocki et al., 2009; Wang et al., 2011; Yu et al., 2008). The permeability of BBB is increased by MMP-9, a major form of gelatinase that degrades extracellular-matrix and tight-junction proteins (Rosell et al., 2008). The MMP-9 gene promoter contains putative nuclear factor-κB (NF-κB) p65 binding sites, and inhibition of NF-κB following ischemic insult blocks MMP-9 gene expression (Cheng et al., 2006; Van den Steen et al., 2002; Wang et al., 2011). In the same way, lithium administered following TBI might induce suppression of neuroinflammation by inhibiting activation of NF-κB, which in turn reduces the upregulation of MMP-9 and disruption of the BBB.

TBI frequently results in behavioral deficits in motor and cognitive function (Fujimoto et al., 2004). In our study, lithium markedly suppressed both short-term and long-term motor deficits in rotarod and beam-walk performance after TBI. Lithium attenuated anxiety-like behavior, as measured by the time spent in the center zone in an open-field test. Our results in the open-field test further showed that lithium treatment attenuated TBI-induced hyper-locomotor activity, a behavior generally interpreted as a sign of depression in mice (Pandey et al., 2009). Accumulating evidence suggests that the hippocampal dentate gyrus is involved in neurogenesis and regulation of behaviors associated with anxiety and depression in rodents (Adachi et al., 2008; Omata et al., 2011). In the present study, we found that lithium attenuated neuronal degeneration in the hippocampal dentate gyrus after TBI. We therefore suggest that the apparent anxiolytic and antidepressant-like effects of lithium stem from its ability to attenuate neurodegeneration in this brain region.

GSK-3, consisting of α and β isoforms, is a serine/threonine kinase involved in diverse cellular functions (Chiu and Chuang, 2010; Li and Jope, 2010; Rowe et al., 2007). Serine phosphorylation of GSK-3β or GSK-3α negatively regulates GSK-3 activity (Chiu and Chuang, 2010; Jope, 1999,2003; Li and Jope, 2010). GSK-3β inhibition or gene silencing effectively suppresses glutamate excitotoxicity in neuronal cultures (Liang and Chuang, 2007). *In vivo* studies found that GSK-3 inhibition reduces infarct volume and improves neurological deficits after cerebral ischemia in rodents (Koh et al., 2008). In a mouse model of TBI, GSK-3 inhibition by lithium is also beneficial in alleviating TBI-induced depressive behavior (Shapira et al., 2007). The effects of GSK-3 inhibition by lithium may be attributable to enhanced expression of important neuroprotective proteins such as heat shock protein 70 (HSP70), BDNF, and Bcl-2 (Liang and Chuang, 2006; Ren et al., 2003; Senatorov et al., 2004; Yasuda et al., 2009). GSK-3 inhibition promotes the activation of cell survival transcription factors, including cyclic adenosine monophosphate response element-binding protein (CREB), AP-1, β-catenin, and heat-shock factor-1 (Bijur and Jope, 2000), and to down-regulate the pro-apoptotic protein p53 and Bax (Chiu and Chuang, 2010; Jope, 2003). These effectors further regulate members of the Bcl-2 protein family, which modulate the balance of cell death and survival signaling (Chiu and Chuang, 2010). GSK-3 has also been shown to crucially regulate immune responses in the CNS (Beurel et al., 2010). Other studies have noted that inhibition of GSK-3 via lithium, as well as other GSK-3 inhibitors, reduces microglial migration, cytokine release, and neurotoxicity (Yuskaitis and Jope, 2009). Notably, GSK-3β and Akt phosphorylation levels increased after TBI (Shapira et al., 2007), and the present study found that there was a trend toward an increase in both p-GSK-3β and p-Akt 3 days after TBI. Lithium treatment robustly increased p-GSK-3β and p-Akt levels, compared with the

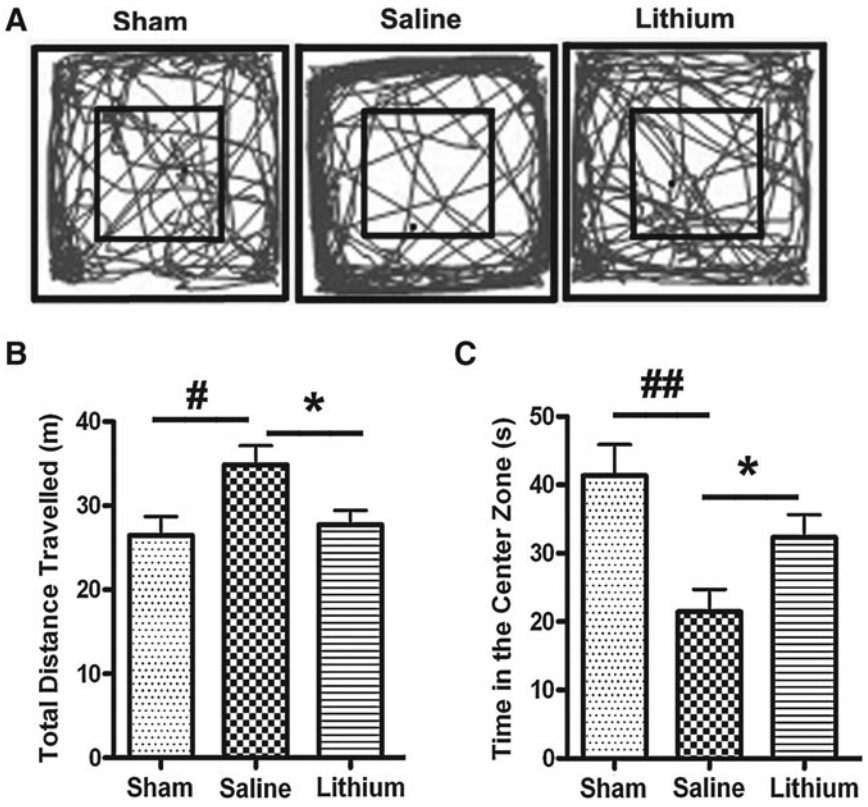

FIG. 7. Lithium attenuates hyper-locomotor activity and anxiety-like behaviors. Representative movement tracks in the open-field test 10 days post-injury in the 2.0 mm group are shown (**A**). The inner square is the center zone of the open field. Traumatic brain injury (TBI) increased gross motor activity and decreased activity in the center zone. The total distance traveled increased in the saline-treated group (**B**; $n=7$ for the sham group; $n=10$ for the saline group; $^{\#}p<0.05$), and significantly decreased in the lithium-treated group (**B**; $n=11$ for the lithium group; $^{*}p<0.05$). The time mice spent in the center zone was significantly reduced in the saline-treated group (**C**; $n=7$ for the sham group; $n=8$ for the saline group; $^{\#\#}p<0.01$), and was significantly increased by lithium treatment (**C**; $n=11$ for the lithium group; $^{*}p<0.05$). Data are represented as mean ± standard error of the mean.

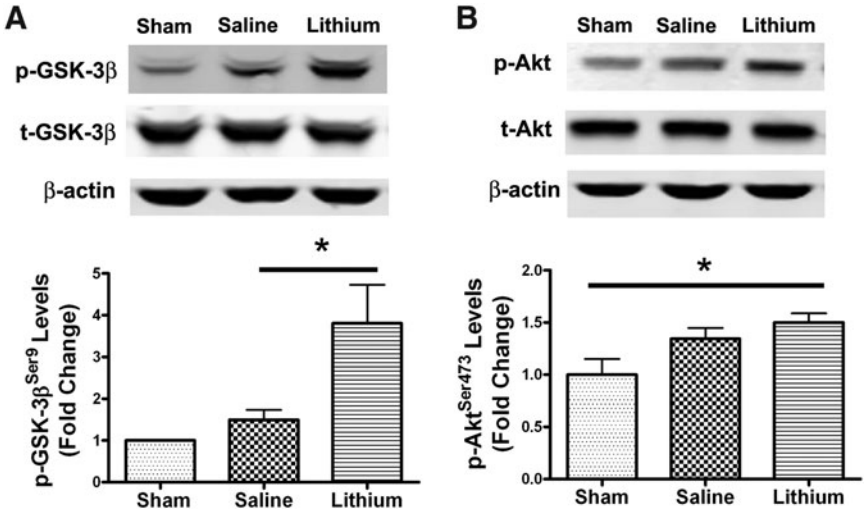

FIG. 8. Lithium increases glycogen synthase kinase-3β (GSK-3β) phosphorylation after traumatic brain injury (TBI). Representative Western blots showed that lithium significantly increased GSK-3β Ser 9 phosphorylation levels 3 days after TBI (**A**). P-GSK-3β levels were slightly increased in the ipsilateral cortex in the saline-treated group compared with the sham-injured group. After lithium treatment, p-GSK-3β levels were markedly increased ($n=6$/group; $^{*}p<0.05$). Representative Western blots showed that lithium increased phosphorylation of Akt Ser 473 (**B**). P-Akt levels had a tendency to increase in the saline-treated group, whereas a significant increase was observed in the lithium-treated group compared with the sham-injured group ($n=5$/group; $^{*}p<0.05$). The levels of total GSK-3β and Akt were unchanged. Levels of β-actin were used as the loading control. Data are represented as mean ± standard error of the mean.

saline-treated and sham-injured groups, respectively. We believe that through GSK-3β inhibition, lithium modulates cell death/survival signaling pathways to reduce cell death. Lithium also suppresses neuroinflammation and reduces neuronal toxicity, which further contributes to neuronal survival. Taken together, lithium reduces lesion volume and attenuates neurodegeneration, leading to the improvement of functional outcome after TBI.

We have reported that long-term pre-insult treatment with lithium is beneficial in an animal model of stroke (Nonaka and Chuang, 1998), suggesting that lithium can be used prophetically in patients with a high risk of stroke such as transient ischemia attack victims. Pre-insult treatment with lithium also has beneficial effects against TBI (Shapira et al., 2007; Zhu et al., 2010). Unlike the case of stroke, the major causes of TBI involve motor vehicle accidents and other unpredicted incidents (Faul et al., 2010). Therefore, it is more clinically relevant to identify the effects of post-insult treatment against TBI. The present study demonstrated multiple beneficial effects of post-insult treatment of lithium, providing a realistic solution to apply this knowledge to the clinical situation.

Based on the results of the present study, we therefore suggest that the neuroprotective, anti-inflammatory, and beneficial behavioral effects of lithium in the TBI mouse model are likely mediated through GSK-3β inhibition and modulation of its downstream effectors. In view of lithium's long history in clinical use, its safety is not in question. Our results that clearly demonstrate its benefits in the mouse model therefore pave the way for early clinical trials as a potential treatment for TBI patients.

Acknowledgments

Support for this work included funding from the Department of Defense in the Center for Neuroscience and Regenerative Medicine, the Blast Lethality Injury and Research Program, and the Intramural Research Program of the National Institute of Mental Health, National Institutes of Health (NIMH-NIH). The authors wish to gratefully acknowledge the editorial assistance of Dr. Elizabeth Sherman, Ioline Henter, and Peter Leeds of the NIMH. We are also grateful to Dr. Oz Malkesman, Laura Tucker, and Dr. Amanda Fu from the Center for Neuroscience and Regenerative Medicine for help with behavioral tests and CCI surgery.

Author Disclosure Statement

No competing financial interests exist.

References

Adachi, M., Barrot, M., Autry, A.E., Theobald, D., and Monteggia, L.M. (2008). Selective loss of brain-derived neurotrophic factor in the dentate gyrus attenuates antidepressant efficacy. Biol. Psychiatry 63, 642–649.

Ahmad, M., Rose, M.E., Vagni, V., Griffith, R.P., Dixon, C.E., Kochanek, P.M., Hickey, R.W., and Graham, S.H. (2008). Genetic disruption of cyclooxygenase-2 does not improve histological or behavioral outcome after traumatic brain injury in mice. J. Neurosci. Res. 86, 3605–3612.

Andreasson, K. (2010). Emerging roles of PGE2 receptors in models of neurological disease. Prostaglandins Other Lipid Mediat. 91, 104–112.

Beaulieu, J.M., Sotnikova, T.D., Yao, W.D., Kockeritz, L., Woodgett, J.R., Gainetdinov, R.R., and Caron, M.G. (2004). Lithium antagonizes dopamine-dependent behaviors mediated by an AKT/glycogen synthase kinase 3 signaling cascade. Proc. Natl. Acad. Sci. USA 101, 5099–5104.

Beurel, E., Michalek, S.M., and Jope, R.S. (2010). Innate and adaptive immune responses regulated by glycogen synthase kinase-3 (GSK3). Trends Immunol. 31, 24–31.

Bijur, G.N., and Jope, R.S. (2000). Opposing actions of phosphatidylinositol 3-kinase and glycogen synthase kinase-3beta in the regulation of HSF-1 activity. J. Neurochem. 75, 2401–2408.

Bramlett, H.M., and Dietrich, W.D. (2007). Progressive damage after brain and spinal cord injury: pathomechanisms and treatment strategies. Prog. Brain Res. 161, 125–141.

Cernak, I., O'Connor, C., and Vink, R. (2002). Inhibition of cyclooxygenase 2 by nimesulide improves cognitive outcome more than motor outcome following diffuse traumatic brain injury in rats. Exp. Brain Res. 147, 193–199.

Chalecka-Franaszek, E., and Chuang, D.M. (1999). Lithium activates the serine/threonine kinase Akt-1 and suppresses glutamate-induced inhibition of Akt-1 activity in neurons. Proc. Natl. Acad. Sci. USA 96, 8745–8750.

Cheng, T., Petraglia, A.L., Li, Z., Thiyagarajan, M., Zhong, Z., Wu, Z., Liu, D., Maggirwar, S.B., Deane, R., Fernandez, J.A., LaRue, B., Griffin, J.H., Chopp, M., and Zlokovic, B.V. (2006). Activated protein C inhibits tissue plasminogen activator-induced brain hemorrhage. Nat. Med. 12, 1278–1285.

Chiu, C.T., and Chuang, D.M. (2010). Molecular actions and therapeutic potential of lithium in preclinical and clinical studies of CNS disorders. Pharmacol. Ther. 128, 281–304.

Chuang, D.M., and Manji, H.K. (2007). In search of the Holy Grail for the treatment of neurodegenerative disorders: has a simple cation been overlooked? Biol. Psychiatry 62, 4–6.

Clausen, F., Hanell, A., Bjork, M., Hillered, L., Mir, A.K., Gram, H., and Marklund, N. (2009). Neutralization of interleukin-1beta modifies the inflammatory response and improves histological and cognitive outcome following traumatic brain injury in mice. Eur. J. Neurosci. 30, 385–396.

Dash, P.K., Orsi, S.A., Zhang, M., Grill, R.J., Pati, S., Zhao, J., and Moore, A.N. (2010). Valproate administered after traumatic brain injury provides neuroprotection and improves cognitive function in rats. PLoS One 5, e11383.

Faul, M., Xu, L., Wald, M.M., and Coronado, V.G. (2010). Traumatic brain injury in the United States: emergency department visits, hospitalization, and deaths. Centers for Disease Control and Prevention, National Center for Injury Prevention and Control: Atlanta.

Fox, G.B., Fan, L., Levasseur, R.A., and Faden, A.I. (1998). Sustained sensory/motor and cognitive deficits with neuronal apoptosis following controlled cortical impact brain injury in the mouse. J. Neurotrauma 15, 599–614.

Fujimoto, S.T., Longhi, L., Saatman, K.E., Conte, V., Stocchetti, N., and McIntosh, T.K. (2004). Motor and cognitive function evaluation following experimental traumatic brain injury. Neurosci. Biobehav. Rev. 28, 365–378.

Gao, X., Deng-Bryant, Y., Cho, W., Carrico, K.M., Hall, E.D., and Chen, J. (2008). Selective death of newborn neurons in hippocampal dentate gyrus following moderate experimental traumatic brain injury. J. Neurosci. Res. 86, 2258–2270.

Hall, E.D., Bryant, Y.D., Cho, W., and Sullivan, P.G. (2008). Evolution of post-traumatic neurodegeneration after controlled cortical impact traumatic brain injury in mice and rats

as assessed by the de Olmos silver and fluorojade staining methods. J. Neurotrauma 25, 235–247.

Hall, E.D., Vaishnav, R.A., and Mustafa, A.G. (2010). Antioxidant therapies for traumatic brain injury. Neurotherapeutics 7, 51–61.

Jope, R.S. (1999). Anti-bipolar therapy: mechanism of action of lithium. Mol. Psychiatry 4, 117–128.

Jope, R.S. (2003). Lithium and GSK-3: one inhibitor, two inhibitory actions, multiple outcomes. Trends Pharmacol. Sci. 24, 441–443.

Kelso, M.L., Scheff, S.W., Pauly, J.R., and Loftin, C.D. (2009). Effects of genetic deficiency of cyclooxygenase-1 or cyclooxygenase-2 on functional and histological outcomes following traumatic brain injury in mice. BMC Neurosci. 10, 108.

Kim, H.J., Rowe, M., Ren, M., Hong, J.S., Chen, P.S., and Chuang, D.M. (2007). Histone deacetylase inhibitors exhibit anti-inflammatory and neuroprotective effects in a rat permanent ischemic model of stroke: multiple mechanisms of action. J. Pharmacol. Exp. Ther. 321, 892–901.

Kirshenboim, N., Plotkin, B., Shlomo, S.B., Kaidanovich-Beilin, O., and Eldar-Finkelman, H. (2004). Lithium-mediated phosphorylation of glycogen synthase kinase-3beta involves PI3 kinase-dependent activation of protein kinase C-alpha. J. Mol. Neurosci. 24, 237–245.

Klein, P.S., and Melton, D.A. (1996). A molecular mechanism for the effect of lithium on development. Proc. Natl. Acad. Sci. USA 93, 8455–8459.

Koh, S.H., Yoo, A.R., Chang, D.I., Hwang, S.J., and Kim, S.H. (2008). Inhibition of GSK-3 reduces infarct volume and improves neurobehavioral functions. Biochem. Biophys. Res. Commun. 371, 894–899.

Kunz, T., Marklund, N., Hillered, L., and Oliw, E.H. (2002). Cyclooxygenase-2, prostaglandin synthases, and prostaglandin H2 metabolism in traumatic brain injury in the rat. J. Neurotrauma 19, 1051–1064.

Kunz, T., Marklund, N., Hillered, L., and Oliw, E.H. (2006). Effects of the selective cyclooxygenase-2 inhibitor rofecoxib on cell death following traumatic brain injury in the rat. Restor. Neurol. Neurosci. 24, 55–63.

Liang, M.H., and Chuang, D.M. (2006). Differential roles of glycogen synthase kinase-3 isoforms in the regulation of transcriptional activation. J. Biol. Chem. 281, 30479–30484.

Liang, M.H., and Chuang, D.M. (2007). Regulation and function of glycogen synthase kinase-3 isoforms in neuronal survival. J. Biol. Chem. 282, 3904–3917.

Loane, D.J., and Faden, A.I. (2010). Neuroprotection for traumatic brain injury: translational challenges and emerging therapeutic strategies. Trends Pharmacol. Sci. 31, 596–604.

Loane, D.J., Pocivavsek, A., Moussa, C.E., Thompson, R., Matsuoka, Y., Faden, A.I., Rebeck, G.W., and Burns, M.P. (2009). Amyloid precursor protein secretases as therapeutic targets for traumatic brain injury. Nat. Med. 15, 377–379.

Lotocki, G., Vaccari, J.P., Perez, E.R., Sanchez-Molano, J., Furones-Alonso, O., Bramlett, H.M., and Dietrich, W.D. (2009). Alterations in blood-brain barrier permeability to large and small molecules and leukocyte accumulation after traumatic brain injury: effects of post-traumatic hypothermia. J. Neurotrauma 26, 1123–1134.

Li, X., and Jope, R.S. (2010). Is glycogen synthase kinase-3 a central modulator in mood regulation? Neuropsychopharmacology 35, 2143–2154.

Maas, A.I., Stocchetti, N., and Bullock, R. (2008). Moderate and severe traumatic brain injury in adults. Lancet Neurol. 7, 728–741.

Margulies, S., and Hicks, R. (2009). Combination therapies for traumatic brain injury: prospective considerations. J. Neurotrauma 26, 925–939.

Niwa, K., Araki, E., Morham, S.G., Ross, M.E., and Iadecola, C. (2000). Cyclooxygenase-2 contributes to functional hyperemia in whisker-barrel cortex. J. Neurosci. 20, 763–770.

Nonaka, S., and Chuang, D.M. (1998). Neuroprotective effects of chronic lithium on focal cerebral ischemia in rats. Neuroreport 9, 2081–2084.

Omata, N., Chiu, C.T., Moya, P.R., Leng, Y., Wang, Z., Hunsberger, J.G., Leeds, P., and Chuang, D.M. (2011). Lentivirally mediated GSK-3beta silencing in the hippocampal dentate gyrus induces antidepressant-like effects in stressed mice. Int. J. Neuropsychopharmacol. 14, 711–717.

Pandey, D.K., Yadav, S.K., Mahesh, R., and Rajkumar, R. (2009). Depression-like and anxiety-like behavioural aftermaths of impact accelerated traumatic brain injury in rats: a model of comorbid depression and anxiety? Behav. Brain Res. 205, 436–442.

Prut, L., and Belzung, C. (2003). The open field as a paradigm to measure the effects of drugs on anxiety-like behaviors: a review. Eur. J. Pharmacol. 463, 3–33.

Quiroz, J.A., Machado-Vieira, R., Zarate, C.A., Jr., and Manji, H.K. (2010). Novel insights into lithium's mechanism of action: neurotrophic and neuroprotective effects. Neuropsychobiology 62, 50–60.

Ren, M., Senatorov, V.V., Chen, R.W., and Chuang, D.M. (2003). Postinsult treatment with lithium reduces brain damage and facilitates neurological recovery in a rat ischemia/reperfusion model. Proc. Natl. Acad. Sci. USA 100, 6210–6215.

Rosell, A., Cuadrado, E., Ortega-Aznar, A., Hernandez-Guillamon, M., Lo, E.H., and Montaner, J. (2008). MMP-9-positive neutrophil infiltration is associated to blood-brain barrier breakdown and basal lamina type IV collagen degradation during hemorrhagic transformation after human ischemic stroke. Stroke 39, 1121–1126.

Rowe, M.K., Wiest, C., and Chuang, D.M. (2007). GSK-3 is a viable potential target for therapeutic intervention in bipolar disorder. Neurosci. Biobehav. Rev. 31, 920–931.

Sassi, R.B., Nicoletti, M., Brambilla, P., Mallinger, A.G., Frank, E., Kupfer, D.J., Keshavan, M.S., and Soares, J.C. (2002). Increased gray matter volume in lithium-treated bipolar disorder patients. Neurosci. Lett. 329, 243–245.

Senatorov, V.V., Ren, M., Kanai, H., Wei, H., and Chuang, D.M. (2004). Short-term lithium treatment promotes neuronal survival and proliferation in rat striatum infused with quinolinic acid, an excitotoxic model of Huntington's disease. Mol. Psychiatry 9, 371–385.

Shapira, M., Licht, A., Milman, A., Pick, C.G., Shohami, E., and Eldar-Finkelman, H. (2007). Role of glycogen synthase kinase-3beta in early depressive behavior induced by mild traumatic brain injury. Mol. Cell. Neurosci. 34, 571–577.

Shein, N.A., Grigoriadis, N., Alexandrovich, A.G., Simeonidou, C., Lourbopoulos, A., Polyzoidou, E., Trembovler, V., Mascagni, P., Dinarello, C.A., and Shohami, E. (2009). Histone deacetylase inhibitor ITF2357 is neuroprotective, improves functional recovery, and induces glial apoptosis following experimental traumatic brain injury. FASEB J. 23, 4266–4275.

Shlosberg, D., Benifla, M., Kaufer, D., and Friedman, A. (2010). Blood-brain barrier breakdown as a therapeutic target in traumatic brain injury. Nat. Rev. Neurol. 6, 393–403.

Van den Steen, P.E., Dubois, B., Nelissen, I., Rudd, P.M., Dwek, R.A., and Opdenakker, G. (2002). Biochemistry and molecular biology of gelatinase B or matrix metalloproteinase-9 (MMP-9). Crit. Rev. Biochem. Mol. Biol. 37, 375–536.

Walker, C.T., Marky, A.H., Petraglia, A.L., Ali, T., Chow, N., and Zlokovic, B.V. (2010). Activated protein C analog with reduced anticoagulant activity improves functional recovery and reduces bleeding risk following controlled cortical impact. Brain Res 1347, 125–131.

Wang, Z., Leng, Y., Tsai, L.K., Leeds, P., and Chuang, D.M. (2011). Valproic acid attenuates blood-brain barrier disruption in a rat model of transient focal cerebral ischemia: the roles of HDAC and MMP-9 inhibition. J. Cereb. Blood Flow Metab. 31, 52–57.

Yasuda, S., Liang, M.H., Marinova, Z., Yahyavi, A., and Chuang, D.M. (2009). The mood stabilizers lithium and valproate selectively activate the promoter IV of brain-derived neurotrophic factor in neurons. Mol. Psychiatry 14, 51–59.

Yu, F., Kamada, H., Niizuma, K., Endo, H., and Chan, P.H. (2008). Induction of mmp-9 expression and endothelial injury by oxidative stress after spinal cord injury. J. Neurotrauma 25, 184–195.

Yu, I., Inaji, M., Maeda, J., Okauchi, T., Nariai, T., Ohno, K., Higuchi, M., and Suhara, T. (2010). Glial cell-mediated deterioration and repair of the nervous system after traumatic brain injury in a rat model as assessed by positron emission tomography. J. Neurotrauma 27, 1463–1475.

Yuskaitis, C.J., and Jope, R.S. (2009). Glycogen synthase kinase-3 regulates microglial migration, inflammation, and inflammation-induced neurotoxicity. Cell Signal. 21, 264–273.

Zhu, Z.F., Wang, Q.G., Han, B.J., and William, C.P. (2010). Neuroprotective effect and cognitive outcome of chronic lithium on traumatic brain injury in mice. Brain Res. Bull. 83, 272–277.

Address correspondence to:
De-Maw Chuang, Ph.D.
Section on Molecular Neurobiology
National Institute of Mental Health
National Institutes of Health
10 Center Drive, MSC-1363
Bethesda, MD 20892-1363

E-mail: chuang@mail.nih.gov

or

Yumin Zhang, M.D., Ph.D.
Department of Anatomy, Physiology, and Genetics
Uniformed Services University of the Health Sciences
4301 Jones Bridge Road
Bethesda, MD 20814

E-mail: yzhang@usuhs.mil